Available online www.jocpr.com

Journal of Chemical and Pharmaceutical Research, 2015, 7(7):1020-1036

Research Article

ISSN : 0975-7384
CODEN(USA) : JCPRC5

Biosynthesis of gold nanoparticles using Marine *Streptomyces cyaneus* and their antimicrobial, antioxidant and antitumor (*in vitro*) activities

El-Batal A. I.[1] and Mona S. S. Al Tamie[2]

[1]*Drug Radiation Research Department, National Center for Radiation Research and Technology (NCRRT), Cairo, Egypt*
[2]*Biology Department, College of Science, Qassim University, Saudi Arabia*

ABSTRACT

The actinobacterial biosynthesis of gold nanoparticles (AuNPs) has been proposed as a cost effective environmental friendly alternative to chemical and physical methods. It is a reliable, important aspect of green chemistry approach that interconnects microbial biotechnology and nanobiotechnology. The target of the present investigation was to optimize the fermentation parameters controlling bioactive metabolites productivity by marine Streptomyces cyaneus, such as certain environmental conditions (different incubation periods, pH values, aeration, shaking speed and inoculum size). Also, by supplying certain nutritional requirements (different carbon and nitrogen sources) for attaining the maximal antimicrobial activity yield by Streptomyces cyaneus against some pathogenic microorganisms. AuNPs were biosynthesized from chloroauric acid using cell free supernatant (as reducing and stabilizing agents), of Streptomyces cyaneus which grown in optimized fermentation medium, by heating or gamma irradiation processes. The synthesized AuNPs were characterized by UV-Vis spectroscopy, Dynamic Light Scattering (DLS), transmission electron microscopy (TEM), X-ray diffraction (XRD) and Fourier transform infrared (FT-IR) spectroscopy, analysis which revealed morphology of spherical AuNPs within nano range from 6.5 nm to 20.0 nm with the main diameter of 12.63 nm by using gamma irradiation at 1 kGy. The biosynthesized AuNPs exhibited good antibacterial activity against some pathogenic Gram positive and Gram negative bacteria, also anti candida. AuNPs exhibited antioxidant activity and antitumor activity against human breast and liver carcinoma cells (in vitro). Finally, Gamma irradiation which induced AuNPs synthesis by cell-free supernatant of Streptomyces cyaneus with improved biomedical different applications is a simple, clean, economic and environmental friendly approach.

Keywords: Gold nanoparticles, *Streptomyces cyaneus*, gamma irradiation, antibacterial, antioxidant and antitumor activities.

INTRODUCTION

Nanotechnology research is one of the major emerging areas of research with its application in science and technology for the purpose of manufacturing new materials at the nanoscale level. Marine nanobiotechnology is one of the fastest growing interdisciplinary fields of research interlacing bionanoscience, biomaterial science and technology, with an exponential progress in biomedical applications such as imaging, diagnostics, drug delivery and therapeutics using metal nanoparticles [1]. Biological synthesis of nanoparticles appears as a suitable process since it requires less energy, is environmentally safe [2], it has low manufacture costs of scalability, and better nanoparticle stabilization, compared to chemically synthesized nanoparticles [3].

Actinobacteriology is one of the important emerging areas of research in tropics. Recent studies of marine microorganisms in the synthesis of nanoparticles are an exciting and upcoming area of research with considerable potential for development [4]. Increasing awareness towards bionanomaterials and other biological processes has

led to the development of simple, eco-friendly and novel biological approaches towards the synthesis of advanced nano biomaterials [5]. It is only recently that biomaterials researchers have proposed marine microorganisms as possible eco-friendly nanofactories for biosynthesis of nanoparticles such as gold [6] and silver [7&8]. Among the actinobacteria, streptomycetes group is considered most economically important because, out of the approximately more than 10 000 known antibiotics, 50–55% is produced by *Streptomyces* [9].

Recently, gold nanoparticles have become the focus of intensive research owing to their wide range of biological and biomedical applications including catalysis, optics, antimicrobials, and the biomaterial production [10]. Gold nanoparticles (AuNPs) are well-suited for a wide range of biological applications because of their unique physical and chemical properties. The marine microbial-mediated synthesis of bionanomaterials has recently been recognized as a potential source for mining bio nanomaterials [11]. Biosynthesis of gold nanoparticles (AuNPs) using bacteria, actinobacteria, fungi and plants [12] are already well documented. However, exploration of the marine actinobacteria has recently heightened interest in the biosynthesis of nanoparticles as nano factories[11]. Recently, actinobacteria isolated from different ecosystems were recognized as potential syntheses of gold and silver bionanoparticles. The biosynthesis and characterization of nanoparticles have only been reported for Thermomonospora sp. [6], *Rhodococcus* sp. [13], *Nocardiopsis* sp. [14] and *Streptomyces* sp. [7&15]. Gold nanoparticles have unique optical properties such as surface-plasmon and photothermal effects. Such properties have resulted in gold nanoparticles having several clinical applications.

Therefore, the purpose of the present work was optimization of the initial composition of the fermentation parameters controlling bioactive metabolites productivity by marine *Streptomyces cyaneus* strain Alex-SK121. The synthesized AuNPs using cell free supernatant, were characterized by UV-Vis spectroscopy, Dynamic Light Scattering (DLS), transmission electron microscopy (TEM) , X-ray diffraction (XRD) and Fourier transform infrared (FT-IR) spectroscopy, analysis. The antimicrobial, antioxidant and antitumor activities of the produced gold nanoparticles were checked.

EXPERIMENTAL SECTION

Chemicals

All the media components from (Oxoid) and (Difco). Chemicals and reagents used in the following experiments were of analytical grade and used without further purification.

Actinobacterium isolate.

In the present study, the cell-free supernatant of *Streptomyces cyaneus* strain Alex-SK121 isolated from sediment samples collected from Sidi Kerir region, Alexandria governorate, Egypt, was found to reduce Au^{3+} ions to AuNPs (gold nanoparticles). Identification and the cultural characteristics of the producer strain were studied through the *International Streptomyces Project* (ISP) [16] and performed according to spore morphology and cell wall chemo-type, which suggested that this strain is Streptomyces. Further cultural, physiological characteristics and analysis of the nucleotide sequence of 16S rRNA gene which were deposited at Gene Bank database (NCBI) under accession number KJ726667 indicated that this strain is identical to *Streptomyces cyaneus* and then designated *Streptomyces cyaneus* strain Alex-SK121 [7].

Parameters controlling bioactive metabolite(s) productivity by *Streptomyces cyaneus*, Alex-SK121.

Effect of certain environmental conditions on the active metabolite productivity by *Streptomyces cyaneus*, Alex-SK121.

A. Effect of different incubation periods.

For such a purpose the spores of culture were allowed to grow on a basal inorganic salt starch nitrate medium [17], in g/l (soluble starch 20, $NaNO_3$ 2, K_2HPO_4 1, KCl 0.5, $MgSO_4.7H_2O$ 0.5, $CaCO_3.2H_2O$ 2 and Tap water up to 1000 ml). The initial pH value of the medium was adjusted at 7.5 -8.0 before sterilization. One hundred ml of the medium was dispensed among conical flasks of 250 ml capacity. Three flasks were used for each particular incubation period. The flasks were then sterilized, cooled, inoculated with inoculum size (5 culture discs , about $1\text{-}3\times10^6$ spores/disc) and incubated on a rotary shaker of 200 rpm. at 36°C. Cultures were removed after 5, 6, 7, 8, 9 and 10 days of incubation and tested for antimicrobial agent(s) biosynthesis.

B. Effect of different pH values.

For such a purpose the initial pH values of the medium were adjusted to cover the range from 6 up to 11 before sterilization. Three flasks were always used for each particular pH value. The experiment was terminated after maximum biosynthesis of metabolite was attained and the broth filtrate was used for antimicrobial potency assessment.

C. Effect of different incubation Temperatures.
The medium were inoculated as previously mentioned and incubated at different temperatures 33^0C, 36^0C, 38^0C and 40^0C the active metabolite productivity was assessed at each particular degree of temperature.

D. Effect of different relative volume capacity (Aeration).
For the detection of a suitable relative volume capacity for maximizing active metabolite the spores of cultures were allowed to grow on a basal inorganic salt starch nitrate medium. The initial pH value of the medium was adjusted at optimum pH before sterilization. Change in the volume of the production medium (20%, 25%, 35%, 40% and 50 %) in flask volume of 250 ml (100%), was performed. The flasks were then sterilized, cooled, inoculated and incubated on a rotary shaker of 200 rpm at optimum temperature. Cultures were removed after optimum incubation periods and tested for antimicrobial agent(s) biosynthesis.

E. Effect of different shaking speed (rpm).
For the detection of a suitable rotation speed (rpm) in shaking conditions for maximizing active metabolite productivity by the isolate. It was allowed to grow on production medium adjusted at optimum pH and incubated at optimum temperature for optimum incubation periods with optimum oxygen content and change in rotation speed, (static) 0, 180,200,220 and 250 rpm was performed. The flasks were then incubated on a shaker incubator where, at the end of optimum incubation period the cultures were removed and tested for antimicrobial agent(s) biosynthesis.

F. Effect of different inoculum size.
For the detection of the optimum inoculum size for maximizing active metabolite productivity, the isolate was allowed to grow on production medium adjusted at optimum pH and incubated at optimum temperature for optimum incubation periods with optimum oxygen content and optimum rpm , change in the number of inoculum size (1,2,3,4,5,6,7and 8) agar culture discs of the isolate, about $1\text{-}3\times10^6$ spores/disc . At the end of optimum incubation period cultures were removed and tested for antimicrobial agent(s) biosynthesis.

Effect of supplying certain nutritional requirements for attaining the maximal antimicrobial yield by *Streptomyces cyaneus*, Alex-SK121:
A. Effect of different carbon sources.
Starch nitrate medium lacking its carbon sources was supplemented with different types of sugars at equimolecular amounts of carbon sources. The carbon sources were represented by, soluble starch, glucose, sucrose, cellulose, xylose and mannitol 2.0 g/100 ml. The sugars under test were separately sterilized and then added separately to the constituents of the inorganic salt starch nitrate medium. The experiment was terminated after the maximum biosynthesis of metabolite was attained and the broth filtrate was then used for assessing the antimicrobial productivity.

B. Effect of different concentrations of the best carbon source.
In this study, different concentrations of the selected carbon source that fulfill the maximum antimicrobial agent biosynthesis were added to the production medium as follows: 1%, 2%, 3%, 4% and 5%.

C. Effect of different nitrogen sources.
The following nitrogenous compounds (yeast extract, peptone, urea, $(NH_4)_2SO_4$ and $NaNO_3$), were supplemented to the inorganic salt starch nitrate medium lacking nitrogen sources. The nitrogen sources were added in an equimolecular amount of nitrogen (N) content of 0.2% for each.

D. Effect of different concentrations of the best nitrogen source.
Different concentrations of the selected nitrogen sources that fulfill the maximum antimicrobial agent biosynthesis was added to the nutrient medium as follows : 0.1%, 0.15%, 0.2%, 0.25%, 0.3%, and 0.35%. (N) contents.

Irradiation Source
The process of irradiation was carried out at the National Center for Radiation Research and Technology (NCRRT) using Cobalt 60 source (Gamma cell 4000-A-India) at a dose rate of 2.08 kGy/h at the time of the experiments

Synthesis and Characterization of gold Nanoparticles (AuNPs).
Cell-free supernatant produced by *Streptomyces cyaneus* Strain Alex-SK121 of optimum medium was mixed with 1mM or more of gold chloride ($HAuCl_4$) solution in ratio of (1:5) (v/v) and were irradiated at ambient temperature with different gamma radiation doses,(un-irradiated, control), 0.5, 1.0, 5.0, 10.0 and 15.0 kGy. They were exposed for different times according to the dose and dose rate. Also, effect of heat on AuNPs synthesis was studied by applying different temperatures such as, 25.0, 50.0, 75.0 and 100 ^{0}C [18-21].

UV-Visible Spectrophotometer (UV-Vis.)
UV-Vis. Spectra of AuNPs were recorded as a function of wave length using JASCO V-560. UV-Vis. Spectrophotometer from 200-900 nm at a resolution of 1 nm and using a filtrate (which contain melanin and the other active supernatant constituents without gold chloride addition) as a base line blank.

Dynamic Light Scattering (DLS)
Average particle size and size distribution were determined by PSS-NICOMP 380-ZLS particle sizing system St. Barbara, California, USA. Before measurements the samples were diluted 10 times with deionized water. 250µl of suspension were transferred to a disposable low volume cuvette. After equilibration to a temperature 25ºC for 2 min, five measurements were performed using 12 runs of 10 s each.

Fourier Transform Infrared Spectrometer (FT-IR)
FT-IR measurements were carried out in order to obtain information about chemical groups present around AuNPs for their stabilization and conclude the transformation of functional group due to reduction process. The measurements were carried out using JASCO FT-IR-3600 infra-red spectrometer by employing KBr Pellet technique.

Transmission Electron Microscopy (TEM)
The size and morphology of the synthesized gold nanoparticles were recorded by using TEM model JEOL electron microscopy JEM-100 CX. TEM studies were prepared by drop coating gold nanoparticles onto carbon-coated TEM grids. The Film on the TEM grids were allowed to dry, the extra solution was removed using a blotting paper.

X-Ray Diffraction (XRD)
X-Ray Diffraction patterns were obtained with The XRD- 6000 series, including stress analysis, residual austenite quantitation, crystallite size/lattice strain, crystallinity calculation, materials analysis via overlaid X-ray diffraction patterns Shimadzu apparatus using nickel-filter and Cu-Ka target, Shimadzu Scientific Instruments (SSI) ,Kyoto, Japan. The average crystalline size of the gold nanoparticles can also be determined using Debye-Scherrer equation : $\mathbf{D = k\lambda / \beta\ Cos\ \theta}$. Where, **D** is the average crystalline size (nm), **k** is the Scherrer constant with value from 0.9 to 1 , λ is the X-ray wavelength , β is the full width of half maximum and θ is the Bragg diffraction angle (degrees).

Atomic Absorption Spectrophotometry
Gold nanoparticles (AuNPs) concentration assessment using UNICAM939 Atomic Absorption Spectrophotometry, England, equipped with deuterium background correction. All solutions were prepared with ultra-pure water.

Melanin estimation
Melanin pigment was estimated from optimized medium according to [22].

Antimicrobial activity of AuNPs.
The biosynthesized active agent(s) and AuNPs were tested for their antimicrobial activity by the agar well diffusion method against different kinds of pathogenic microbial strains of Gram-positive bacteria (*Bacillus subtilis* ATCC 6633 and *Staphylococcus aureus* ATCC 6538) and Gram-negative bacteria (*Escherichia coli* ATCC 7839 and *Pseudomonas aeruginosa* ATCC 9027), also against unicellular fungi (*Candida albicans* ATCC 10231) according to the method of [23]. The growth inhibition of microbial pathogens was assessed by the corresponding zone of inhibition (ZOI) [24]. Sterile standard antibiotic disks with diameter of 6 mm were used to evaluate the activity of the synthesized AuNPs. The pure cultures of bacteria and fungi were subcultured on Muller-Hinton (Oxoid) broth for bacteria and Sabouraud broth for fungi at 37 ^{0}C and 30 ^{0}C on a rotary shaker at 180 rpm, respectivily. Wells of 6 mm diameter were made on Muller-Hinton Agar and Sabouraud agar plates using gel puncture. Each strain was swabbed uniformly onto the individual plates using sterile cotton swabs and incubated at optimum condtions for tested bacteria and fungi and ZOI was measured using a Vernier caliper (mm).

Determination of minimum inhibitory concentration (MIC)
The minimum inhibitory concentrations (MIC) determination were performed in Luria Bertani (LB) broth in duplicate using serial two-fold dilutions of AuNPs with positive control well (the microorganism and the nutrient) and negative control one (the nutrient only) [25,26]. The MIC was determined after 24 hrs. of incubation at 37^{0}C with initial inoculums of 0.1 O.D at 600 nm. MIC can determined by using two methods:

a)-Visually by comparison with the cell free filtrate controls.
b)-With ELISA plate reader at a wavelength of 620 nm.

Antioxidant activity assay (Free radical scavenging ability on 2, 2-diphenyl-2-picrylhydrazyl (DPPH), (*In vitro* assay)

Antioxidant activity of the synthesized AuNPs from strain Alex-SK121 was carried out by measuring scavenging activity of 2, 2-diphenylpicrylhydrazyl (DPPH) free radicals according to [18]. In brief, 2 ml of distilled water, 1 ml of 0.1 mM DPPH solution in ethanol and 0.5 ml of the biosynthesized AuNPs were shacked vigorously and allowed to reach a steady stat for 30 min at room temperature. Decolorization of DPPH was determine by measuring the decrease in absorbance at 517nm. The lower absorbance of the reaction mixture indicated a higher percentage of scavenging activity. The percentage of inhibition or scavenging of free radicals was determined by the following Formula :

% Inhibition = [(Control OD - Sample OD)/Control OD] × 100

Where the control was prepared as described above without a sample and tert-Butyl hydroquinone (TBHQ) was compared as standard.

Antitumor Activity of AuNP

Antitumor activity of synthesized AuNPs was carried out by Sulphorodamine B (SRB) assay. In this method, the monolayer cell culture was trypsinized and the cell count was adjusted to 0.5-1.0 x 10^5 cells/ml using medium containing 10% new born sheep serum. To each well of the 96 well micro titre plates, 0.1ml of the diluted cell suspension (approximately 10,000 cells) was added. After 24 hours, when a partial monolayer was formed, the supernatant was flicked off, washed once and 100 µl of different test concentrations were added to the cells in micro titre plates. The plates were then incubated at 37°Cfor 72 hours in 5% CO_2 incubator, microscopic examination was carried out, and observations recorded every 24 hours. After 72 hours, 25 µl of 50% trichloro acetic acid (TCA) was added to the wells gently such that it forms a thin layer over the test compounds to form overall concentration 10%. The plates were incubated at 4°C for one hour.

The plates were flicked and washed five times with sterile water to remove traces of medium, sample and serum, and were then air-dried. The air-dried plates were stained with 100 µl SRB and kept for 30 minutes at room temperature. The unbound dye was removed by rapidly washing four times with 1% acetic acid. The plates were then air dried. 100 µl of 10 mM Tris base was then added to the wells to solubilize the dye. The plates were shaken vigorously for 5 minutes. The absorbance was measured using micro plate reader at a wavelength of 540 nm [27]. The percentage growth inhibition was calculated using following formula,

Percentage of cell viability %= Sample absorbance/ control absorbance × 100

Statistical analysis*:* The means of three replications and standard deviation (SD±) were calculated for all the results obtained, and the data were subjected to analysis of variance [28].

RESULTS AND DISCUSSION

Effect of certain environmental conditions on the active metabolites productivity by *Streptomyces cyaneus*, Alex-SK121.

A. Effect of different incubation periods on the active metabolites productivity by *Streptomyces cyaneus*, Alex-SK121.

This experiment was devoted to detect the suitable incubation period needed for the production of highest yield of active metabolites by *Streptomyces cyaneus*, Alex-SK121. The active metabolites productivity were detected at time intervals of 5, 7, 8, 9 and 10 days on production medium. Time is an important factor to affect the fermentation. Increasing time does not mean producing more secondary metabolites. It may produce more toxins to inhibit the production of antimicrobial metabolites. Data are illustrated in table (1) which showed the relation between active metabolite productivity and time of incubation. The level of the active metabolites yield increased at 5 days and decrease gradually with increasing the incubation period at the end of 10 days. Also, It can be seen that, the fermentation time appeared to have visible effect on the mycelial growth inhibition of *Streptomyces cyaneus*, Alex-SK121 at 7-10 days. According to [29], this is due to the fact that the extent of antimicrobial metabolites production equals the tolerance of the cells to these metabolites. Also, this may be attributed to one of the following factors: a shortage of intermediate precursors which decrease the feedback effect of the accumulated metabolites or the irreversible decay of one or more used enzymes in the biosynthesis process [30].

Table (1): Relation between active metabolites productivity and time of incubation

Different incubation periods(days)	Mean diameter of inhibition zone (mm) of the tested microbial strains with standard deviation(SD±)			Dry weight mg/ml
	B. subtilis ATCC 6633	*E. coli* ATCC 7839	*C. albicans* ATCC 10231	
4	25 ± 2	15 ± 1	17 ± 1	1.1 ± 0.1
5	31 ± 3	22 ± 2	23 ± 2	1.3 ± 0.1
7	28 ± 1	20 ± 2	18 ± 1	1.0 ± 0.2
9	25 ± 2	16 ± 1	16 ± 1	0.9 ± 0.1
10	24 ± 2	15 ± 1	12 ± 1	0.8 ± 0.2

B. Effect of different initial pH values on the active metabolites productivity by *Streptomyces cyaneus,* Alex-SK121

Effect of different initial pH values on the active metabolites produced by *Streptomyces cyaneus*, Alex-SK121 and the final pH values was studied. For this purpose, production medium was adjusted at different initial pH values covering rang of (6 -10) and incubated at 36^{o}C for five days. It could be concluded from the results represented in (table 2) that, the optimum initial pH value capable of promoting active metabolite biosynthesis by *Streptomyces cyaneus*, Alex-SK121 was at the initial value of 9.0 (final pH value, 7.3), since, the activities resulted from active metabolites productivity reached up to 33.0 mm against *B. subtilis* ATCC 6633, below this particular pH value, the active metabolites yield decreased. So, the initial pH value of the present work showed a significant influence on the growth of strain under investigation and consequently on the antimicrobial agent highest yield. Acidic pH inhibited the active metabolite production rather than high alkaline pH. Similar observations were reported by [31] who noticed that pH 7 was the most suitable for large scale production of antibiotics by Streptomyces species.

Table (2): Relation between active metabolites productivity and different pH

Different initial pH values	Mean diameter of inhibition zone (mm) of the tested microbial strains with standard deviation(SD±)			Final pH values	Dry weight mg/ml
	B. subtilis ATCC 6633	*E. coli* ATCC 7839	*C. albicans* ATCC 10231		
6	26 ± 2	23 ± 2	27 ± 1	5.6	0.8 ± 0.0
7	27 ± 2	22 ± 1	19 ± 2	6.1	0.9 ± 0.1
8	30 ± 3	23 ± 2	22 ± 2	6.8	1.2 ± 0.2
9	33 ± 3	25 ± 2	28 ± 3	7.5	1.5 ± 0.2
10	25 ± 2	22± 2	23 ± 2	7.6	1.4 ± 0.3

C. Effect of different incubation temperatures on the active metabolites productivity by *Streptomyces cyaneus,* Alex-SK121.

For the detection of a suitable incubation temperature for maximizing active metabolites productivity by *Streptomyces cyaneus*, Alex-SK121, it was allowed to grow on production medium adjusted at initial pH (9) and incubated at different temperature degrees covering the rang from 33-40 ^{o}C for five days. Data represented in (table 3) showed that, the optimum temperature capable of promoting active metabolites biosynthesis by *Streptomyces cyaneus*, Alex-SK121., was at 38^{o}C where the maximum activities resulted from active metabolite productivity reached up to 34mm against *B.subtilis* ATCC 6633. Below and above this particular temperature degree, active metabolites produced by this strain under investigation, gradually decreased as compared to the optimal temperature. Deviation from optimum temperature affects the efficiency of metabolite. In this connection, [32] showed that temperature is a regulatory factor in the secondary metabolism of *St. thermoviolaceus*.

Table (3): Relation between active metabolites productivity and different temperature

Different incubation temperature	Mean diameter of inhibition zone (mm) of the tested microbial strains with standard deviation(SD±)			Dry weight mg/ml
	B. subtilis ATCC 6633	*E. coli* ATCC 7839	*C. albicans* ATCC 10231	
33^{0}C	24 ± 2	14 ± 1	21 ± 1	1.2 ± 0.1
36^{0}C	32 ± 3	27 ± 2	29 ± 2	1.3 ± 0.1
38^{0}C	34 ± 2	28 ± 2	30 ± 3	1.6 ± 0.2
40^{0}C	26 ± 2	20 ± 2	20 ± 2	1.3 ± 0.2

D. Effect of relative different volume capacity (Aeration) of production medium on the active metabolites productivity by *Streptomyces cyaneus,* Alex-SK121.

For the detection of a suitable relative volume capacity for maximizing active metabolites productivity by *Streptomyces cyaneus*, Alex-SK121, it was allowed to grow on production medium adjusted at initial pH (9) and incubated at 38^{o}C for five days (shaking condition) through change in the volume of the production medium (20%,

25%, 35%, 40% and 50 %) in flask volume of 250 ml (100%). Data represented in (table 4) showed that, the optimum relative volume capacity 40 % capable of promoting active metabolite biosynthesis by *Streptomyces cyaneus*, Alex-SK121.

Table (4): Relation between active metabolite productivity and different volume capacity

Different relative volume capacity %	Mean diameter of inhibition zone (mm) of the tested microbial strains with standard deviation(SD±)			Dry weight mg/ml
	B. subtilis ATCC 6633	*E. coli* ATCC 7839	*C. albicans* ATCC 10231	
20%	10 ± 1	11 ± 1	13 ± 1	0.8 ± 0.1
25%	14 ± 1	13 ± 1	12 ± 1	1.0 ± 0.2
35%	16 ± 1	13 ± 1	14 ± 1	1.2 ± 0.1
40%	35 ± 3	27 ± 2	29 ± 2	1.7 ± 0.2
50%	33 ± 2	28 ± 2	30 ± 3	1.4 ± 0.2

E. Effect of different shaking speed (rpm) on the active metabolites productivity by *Streptomyces cyaneus*, Alex-SK121.

Effect of agitation on production of metabolite was detected at different agitation conditions (static) 0, 180, 200, 220 and 250 rpm in shaking conditions for maximizing active metabolites productivity by *Streptomyces cyaneus*, Alex-SK121. It was allowed to grow on production medium adjusted at initial pH (9) and incubated at 38 ^{o}C for five days shaking condition 100ml (40%) of medium in flask volume of 250 ml (100%). Agitation represented in (table 5) showed direct effect on the growth and active metabolites biosynthesis of *Streptomyces cyaneus*, Alex-SK121 because agitation affects aeration and mixing of the nutrients in the fermentation medium. So, the optimum rpm capable of promoting active metabolites biosynthesis by *Streptomyces cyaneus*, Alex-SK121 was at 200 rpm. These finding agree with the results of [33], who demonstrated that production of antibiotics by *Streptomyces* spp. is generally believed to be an aerobic process. Therefore , dissolved oxygen (DO) is an important factor in the fermentation of *Streptomyces cyaneus*, Alex-SK121. In shaken flasks, oxygen supply is related to medium volume. Otherwise, inoculation volume can affect the metabolites accumulation.

Table (5): Relation between active metabolites productivity and different shaking speed (rpm)

Different shaking speed (rpm)	Mean diameter of inhibition zone (mm) of the tested microbial strains with standard deviation(SD±)			Dry weight mg/ml
	B. subtilis ATCC 6633	*E. coli* ATCC 7839	*C. albicans* ATCC 10231	
(Static) 0	22±2	16±1	22±2	1.9±0.2
180	33 ± 3	25 ± 2	27 ± 2	1.4 ± 0.2
200	36 ± 3	27 ± 2	29 ± 3	1.8 ± 0.1
220	27 ± 2	19 ± 1	21 ± 2	1.1 ± 0.2
250	25 ± 2	17 ± 1	20 ± 2	1.0 ± 0.1

Table(6): Relation between active metabolites productivity and different inoculum size

Inoculum size (No. of discs)	Mean diameter of inhibition zone (mm) of the tested microbial strains with standard deviation(SD±)			Dry weight mg/ml
	B. subtilis ATCC 6633	*E. coli* ATCC 7839	*C. albicans* ATCC 10231	
1	20 ± 1	12 ± 1	15 ± 1	0.8 ± 0
2	20 ± 1	12 ± 1	16 ± 1	0.9 ± 0.1
3	25 ± 2	15 ± 1	18 ± 2	1.0 ± 0.2
4	25 ± 3	17 ± 1	20 ± 2	1.1 ± 0.1
5	34 ± 2	26 ± 3	25 ± 1	1.6 ± 0.1
6	38 ± 3	28 ± 2	30 ± 2	2.1 ± 0.2
7	28 ± 3	20 ± 1	21 ± 2	2.5 ± 0.1
8	28 ± 2	20 ± 2	20 ± 1	2.4 ± 0.2

F. Effect of different inoculum size on the active metabolites productivity by *Streptomyces cyaneus*, Alex-SK121.

For the detection of the optimum inoculum size for maximizing active metabolites productivity by *Streptomyces cyaneus*, Alex-SK121, it was allowed to grow on production medium adjusted at initial pH (9) and incubated at 38 ^{o}C for five days (shaker conditions 120ml in flask 250ml),at 200rpm and change in the number of inoculum size (1, 2, 3, 4, 5, 6, 7 and 8 agar culture disc), about (1-3×10^{6} spores/disc) of *Streptomyces cyaneus*, Alex-SK121. Data represented in (table 6) showed the optimum inoculum size (6 culture discs) capable of promoting active metabolites biosynthesis by *Streptomyces cyaneus*, Alex-SK121. It is interesting to note that, inoculum concentration showed direct effect on the production based on varying inoculum level. A lower inoculum density may reduce product

formation, whereas, a higher inoculum may lead to the poor product formation, especially the large accumulation of toxic substances and also cause the reduction of dissolved oxygen.

Effect of supplying certain nutritional requirements on the active metabolites production by *Streptomyces cyaneus*, Alex-SK121.

A. Effect of supplying different carbon sources on the active metabolites production by *Streptomyces cyaneus*, Alex-SK121.

A study on the production of antibiotics usually involves a search for optimal media costituents. This is achieved by a systematic study of the suitability of a large number of carbon and nitrogen sources. The ability of streptomycete to form antibiotic was not a fixed property but can be greatly increased or completely lost under different conditions of nutrition and cultivation. For the detection of a suitable carbon sources for maximizing the active metabolites productivity by *Streptomyces cyaneus*, Alex-SK121, It was allowed to grow on production medium containing different six carbon sources 2%: soluble starch, sucrose, glucose, cellulose, xylose and mannitol. The choice of carbon source greatly influenced secondary metabolism and therefore antibiotic production [30&34]. Also, a slowly utilizable carbohydrate gave a higher yield of the antibiotic because of its availability in adequate amount during both the phases of cellular growth and antibiotic production. A quickly metabolized substrate such as glucose may often achieved maximum cell growth rates, but it was known to inhibit the production of many secondary metabolites. This catabolite repression was thought to be due to intermediates generated from the rapid catabolism of glucose interfering with enzymes in the secondary metabolism process. Data represented in (table7) showed that, the highest active metabolite productivity by *Streptomyces cyaneus*, Alex-SK121, was obtained in the presence of soluble starch, which was followed by glucose, sucrose and cellulose. Since, the activities resulted from active metabolites productivity in case of soluble starch reached up the highest inhibition zone.

Table (7): Relation between active metabolite productivity and different carbon source

Carbon source (2%)	Mean diameter of inhibition zone (mm) of the tested microbial strains with standard deviation(SD±)			Dry weight mg/ml
	B. subtilis ATCC 6633	*E. coli* ATCC 7839	*C. albicans* ATCC 10231	
Soluble starch	37 ± 2	26 ± 2	29 ± 2	2.0 ± 0.23
Sucrose	30 ± 3	19 ± 2	21 ± 2	1.4 ± 0.1
Glucose	31 ± 3	20 ± 2	23 ± 2	1.7 ± 0.1
Cellulose	17 ± 1	16 ± 1.7	15 ± 1	1.1 ± 0.1
Xylose	14 ± 1	12 ± 1	10 ± 1	1.0 ± 0.1
Mannitol	13 ± 1	11 ± 1	10 ± 1	0.8 ± 0.1

B. Effect of supplying different soluble starch concentrations on the active metabolites yield produced by *Streptomyces cyaneus*, Alex-SK121.

This experiment was performed to detect best soluble starch concentration needed to fulfill maximum active metabolite yield produced by *Streptomyces cyaneus*, Alex-SK121. Different Soluble starch concentrations covering rang of (1%-5%) were employed for this purpose. The results represented in (table 8) showed that, the best concentration of soluble starch was at 2%, while, the antibiotic production decreased at higher concentration. On the other hand, the selected carbon sources were completely consumed when used at this concentration. The higher concentration of carbon source may resulted in the accumulation of this carbon source in the cultivation medium and the remained amount depended on the initial concentration. These results agreed with [35] who reported that increasing concentrations of preferred carbon sources, such as glycerol and maltose, decreased production of the antibiotics.

Table (8): Relation between active metabolites productivity and different soluble starch concentrations

Soluble starch concentrations (%)	Mean diameter of inhibition zone (mm) of the tested microbial strains with standard deviation(SD±)			Dry weight mg/ml
	B. subtilis ATCC 6633	*E. coli* ATCC 7839	*C. albicans* ATCC 10231	
1	26 ± 1	16 ± 1	14 ± 1	1.0 ± 0.1
2	38 ± 4	28± 2	30 ± 2	1.9 ± 0.1
3	30 ± 3	19 ± 1	16 ± 1	1.3 ± 0.1
4	24 ± 2	18 ± 1	18 ± 1	1.2 ± 0.1
5	22 ± 2	18 ± 2	19 ± 2	1.3 ± 0.2

C. Effect of supplying different nitrogen sources on the active metabolites yield produced by *Streptomyces cyaneus*, Alex-SK121.

In a similar way to carbon, the nitrogen source was used to regulate secondary metabolism. For the detection of a suitable nitrogen source for maximizing the active metabolites productivity by *Streptomyces cyaneus*, Alex-SK121, it was allowed to grow on starch nitrate production medium containing different organic and inorganic nitrogen sources as, peptone, urea, sodium nitrate, yeast extract and ammonium sulphate at (0.2 %, N content). The results revealed that the level of the active metabolites production may be greatly influenced by the nature, type and concentration of the nitrogen source supplied in the culture medium. Data represented in (table 9) showed that, the highest active metabolites productivity by *Streptomyces cyaneus*, Alex-SK121, was obtained in the presence of sodium nitrate, this was followed by yeast extract and peptone. Since the activities resulted from active metabolites productivity in case of sodium nitrate reached up highest inhibition zone. These findings agree with the results of [36] who stated that the highest antibiotic production was obtained in cultures containing sodium nitrate or potassium nitrate as a nitrogen source.

Table (9): Relation between active metabolites productivity and different nitrogen sources

Nitrogen source (0.2 %,N content)	Mean diameter of inhibition zone (mm) of the tested microbial strains with standard deviation(SD±)			Dry weight mg/ml
	B. subtilis ATCC 6633	*E. coli* ATCC 7839	*C. albicans* ATCC 10231	
Peptone	25 ±2	16 ± 1	17 ± 1	1.7 ± 0.1
Urea	17 ± 1	14 ± 1	16 ± 1	1.2 ± 0.1
Sodium Nitrate	38 ± 3	30 ± 2	29 ± 2	1.8± 0.2
Yeast extract	27 ± 2	18 ± 1	19 ± 1	1.6 ± 0.1
Ammonium Sulphate	16 ± 1	13 ± 1	14 ± 1	1.1 ± 0.1

D. Effect of supplying different sodium nitrate concentrations on the active metabolites yield produced by *Streptomyces cyaneus*, Alex-SK121.

This experiment was performed to detect best $NaNO_3$ concentration needed to fulfill maximum active metabolites yield produced by *Streptomyces cyaneus*, Alex-SK121. Different $NaNO_3$ concentrations covering rang of (0.1 % - 0.35 %,N content) were employed for this purpose. Results represented in (table 10) showed that, the best concentration of sodium nitrate was at 0.2% N content. High nitrogen levels had been noted to repress iodophase production of antibiotics [34&37]. From the above mentioned pattern of results, it appears that the optimization of fermentation process should be considered not only the reduction of the costs of raw material but also the high antimicrobial activity. In this study the information obtained is useful for developing a *Streptomyces cyaneus*, Alex-SK121 cultivation process for efficient production of antimicrobial active metabolites on a large scale.

Table (10): Relation between active metabolites productivity and different sodium nitrate concentrations

Sodium nitrate Concentrations (% N, content)	Mean diameter of inhibition zone (mm) of the tested microbial strains with standard deviation(SD±)			Dry weight mg/ml
	B. subtilis ATCC 6633	*E. coli* ATCC 7839	*C. albicans* ATCC 10231	
0.1	13 ± 1	16 ± 1	15 ± 1	0.9 ±0.1
0.15	12 ± 1	15 ± 1	14 ± 1	1.5 ± 0.1
0.2	37± 3	29 ± 2	28 ± 3	2.0 ± 0.2
0.25	25 ± 2	19 ± 1	24 ± 2	1.5 ± 0.1
0.3	19 ± 1	16 ± 1	14 ± 4	1.3 ± 0.1
0.35	15 ± 1	18 ± 1	14 ± 1	0.9 ± 0

Microbial Synthesis of gold Nanoparticles

Due to its unique properties, gold nanoparticles (AuNPs) have been used as an additive to various drugs, and are designated as passive medicine. Green synthesis of gold nanoparticles using microorganisms or biologically active metabolites provides advancement over chemical and physical methods as it is cost effective, environment friendly, easily scaled up for large scale synthesis and in this method there is no need to use high pressure, energy, temperature and toxic chemicals.

Therefore, it can be assumed in this study that, the secreted active metabolites in the cell free supernatant such as proteins/enzymes (chitinase, amylase, protease, lipase, catalase, nitrate reductase and tyrosinase) and reducing agents such as amino acids, peptides, organic acids, antimicrobial metabolites and melanin pigments in biological entities, are found to be responsible for nanoparticle production by reducing gold ions into AuNPs. These compounds contain functional groups that play a role in the reduction and hence the synthesis as well as the stabilization of gold nanoparticles. These metabolites create electrostatic attraction of negatively charged chemical

active moieties groups, therefore stabilizing these gold nanoparticles by "capping" to prevent their aggregation through the creation of repulsive forces [7&21&38].

On the other hand, in this study the cell free supernatant of *Streptomyces cyaneus* strain Alex-SK121 was able to synthesis gold nanoparticles when added to the aqueous Au^{3+} ions which reduced to AuNPs, and this is indicated by the color change from pale brown (due to melanin pigment , 2mg/ml supernatant) to dark pink color while control dos not give any color change. Also, the result of AuNPs synthesis at different temperature 25, 50, 75 and 100 ^{0}C indicating that the maximum absorption (1.3) was recorded at 100 ^{0}C as shown in (table 11.)

Based on previous studies [39], the key role of exposing thiol groups of enzymes or other chemical active groups in the metabolites, for AuNPs formation, is high temperature that destructs the appropriate folding of them and exposes hydrophobic and hidden groups with reductive ability and makes them possible to form nanometallic structures. The effect of temperature was determined by carrying out the reaction at different temperatures. It was found that as temperature increases, the AuNPs synthesis rate increases and the time taken for color conversion was much reduced. At room temperature, there was an initial lag period for the formation of AuNPs and the synthesis time was longer, reaching 20 minutes. At 100 ^{0}C, only 2 minutes were required to get the highest absorbance (1.3) indicating the highest productivity of AuNPs, this result was in agreement with previous studies [21].

The radiation induced synthesis is one of the most promising strategies because it is simple, clean and has harmless feature. The irradiated solution at different gamma radiation doses such as 0.5, 1.0, 5.0, 10.0 and 15.0 kGy were then characterized using UV.Vis. Spectrometer. So, the maximum absorption (1.83) was recorded at 1 k Gy as indicating in (table 12.) The formation of AuNPs can be attributed to the radiolytic reduction which generally involves radiolysis of aqueous solutions that provides an efficient method to reduce metal ions. In the radiolytic method, when aqueous solutions are exposed to gamma rays, they create hydrated electrons, produced during the irradiation, which reduce the gold metal ions to zero-valent atoms AuNPs . Also, the possible mechanism suggests that the radiolytic reduction by gamma radiation of aqueous solution is carried out by organic radicals formed. *Streptomyces cyaneus* strain Alex-SK121 supernatant molecules especially pale brown melanin pigments (**$C_{18}H_{10}N_2O_4$**, melanin structure formula), which plays an important role in scavenging the free radicals and converted into organic radicles. It is worth noting that, naked (e.g. uncoated) particles are not stable, therefore AuNPs are commonly protected by stabilizing ligands which found in the supernatant such as melanin pigments and other enzymes as catalases, amylases, lipases, tyrosinase and chitinase. Solubility of AuNPs largely depends on the polarity and hydrophilicity of the protecting ligand. Soluble AuNPs are also known as colloidal gold.

Table 11: Effect of temperature on gold nanoparticles synthesis

Temperature (ºC)	Maximum absorption O.D	Time (minute)	Wavelength(nm)
25	0.4	20	550
50	0.75	5	550
75	0.9	3	550
100	1.3	2	550

Table 12: Effect of gamma irradiation on gold nanoparticles synthesis

Radiation doses (kGy)	Maximum absorption (O.D)	Wavelength (nm)
0.5	0.798	535
1	1.83	525
5	1.52	530
10	1.209	535
15	0.488	540

AuNPs are among the most popular metal nanoparticles due to their stability and fascinating properties. Owing to the good biocompatibility and non-toxic nature of AuNPs, they are widely used in biology and medicine. The appearance of dark pink color in irradiated solution at 1 kGy and heated solution at 100^{o}C suggested the formation of AuNPs and the color change is attributed to the Surface Plasmon Resonance (SPR).The strong interaction of the AuNPs with light occurs because the conduction electrons on the metal surface undergo a collective oscillation when excited by light at specific wavelengths known as a Surface Plasmon Resonance (SPR). The following provisional suggested mechanism for reduction, which is consistent with similar studies on the irradiation reduction of AgNPs and AuNPs in other solutions.

The growth of gold nanoparticles by reduction of Au^{3+} to Au^0 is step wise show in the following Eqs. (1), (2), (3), (4) and (5), according to speculative reduction mechanisms [7&19&40&41].

$$* H_2O \xrightarrow{\text{Gamma-irradiation}} e^-_{aq}, H_3O^+, H^\cdot, OH^\cdot, H_2^\cdot, H_2O_2^\cdot \quad (1)$$

$$*C_{18}H_{10}N_2O_4\ (\text{melanin structure formula}) + OH^\cdot \longrightarrow H_2O + C^\cdot_{18}H_9N_2O_4 \quad (2)$$

A secondary radical is formed **($C^\cdot_{18}H_9N_2O_4$)** which efficiently reduces the precursor metal ions Au^{3+} to Au^0.

$$*C^\cdot_{18}H_9N_2O_4 + Au^{3+} \longrightarrow Au^0 + C_{18}H_8N_2O_4 \quad (3)$$

$$*C^\cdot_{18}H_9N_2O_4 + Au_2^{3+} \longrightarrow Au_2^0 + C_{18}H_7N_2O_4 \quad (4)$$

$$*C_{18}H_9N_2O_4 + Au_n^{3+} \longrightarrow Au_n^0 + C_{18}H_{n-1}N_2O_4 \quad (5)$$

Characterization of the synthesized gold nanoparticles (AuNPs).

Characterization of AuNPs synthesized by cell-free supernatant of *Streptomyces cyaneus* strain Alex-SK121 at 1 kGy of gamma irradiation and heated at 100^{o}C was performed through the following analysis;

UV-Visible Spectrophotometer (UV-Vis.)

The dispersion of gold nanoparticles displays intense colors due to the Plasmon resonance absorption. The surface of a metal is like plasma, having free electrons in the conduction band and positively charged nuclei. Surface Plasmon Resonance (SPR) is a collective excitation of the electrons in the conduction band; near the surface of the nanoparticles. Electrons are limited to specific vibrations modes by the particle's size and shape. Therefore, metallic nanoparticles have characteristic optical absorption spectrum in the UV-Visible region [41]. As shown in Fig.1. UV-Visible spectrum of AuNPs synthesized by heating which indicated that 100^{0}C was the best temperature used in AuNPs synthesis in the presence of cell-free supernatant of *Streptomyces cyaneus* strain Alex-SK121. Also, Fig. 2, showing UV-Visible spectrum of AuNPs Synthesized by gamma irradiation at 1 kGy in the presence of cell-free supernatant of *Streptomyces cyaneus strain* Alex-SK121. it worth mentioning that the specific UV.Visibe spectrum of melanin pigment at ƛ 475 nm not found in Fig. 1&2 because we used the filtrate as a blank as mentioned in materials and methods. The important biomedical applications of AuNPs in different fields originate from their size, versatility and usability.

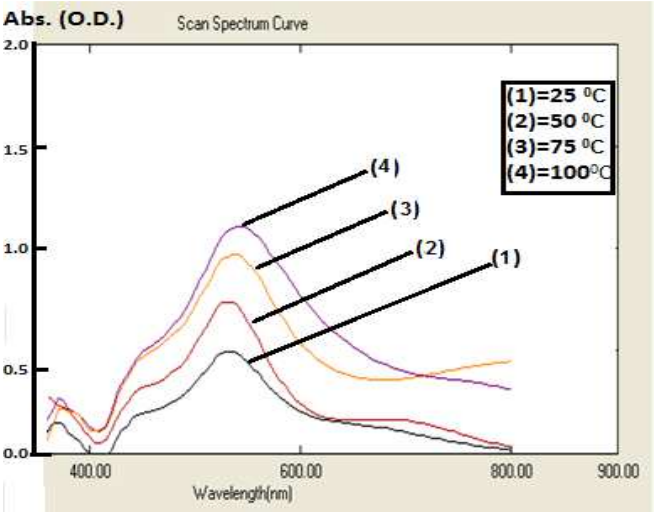

Fig. 1. UV-Visible spectrum of AuNPs synthesized by heating in the presence of cell-free supernatant of *Streptomyces cyaneus* strain Alex-SK121 at different temperature 25.0, 50.0, 75.0 and 100 ^{0}C

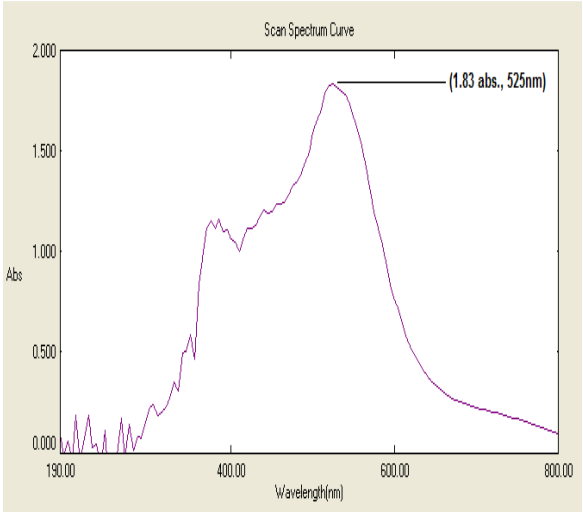

Fig. 2. UV-Visible spectrum of AuNPs synthesized by gamma irradiation in the presence of cell-free supernatant of *Streptomyces cyaneus* strain Alex-SK121 at 1 kGy

Dynamic Light Scattering (DLS)

In order to examine the particles size distribution, DLS was also performed and its results were compared to the TEM data. The average particle size was determined by dynamic light scattering (DLS) method and found to be 33.3 nm (Fig. 3 in AuNPs synthesized by cell-free supernatant of *Streptomyces cyaneus* strain Alex-SK121 and heated at 100^{o}C) and 16.6 nm as shown in (Fig. 4), AuNPs synthesized by cell-free supernatant of *Streptomyces cyaneus* strain Alex-SK121 and gamma irradiated at 1 kGy.

Transmission Electron Microscopy (TEM).

Transmission electron microscopy (TEM) examination of the solution containing AuNPs synthesized in the presence of cell-free supernatant of *Streptomyces cyaneus* strain Alex-SK121 and heated at 100^{o}C which

demonstrated spherical particles within nano ranged from 16.4 nm to 26.6 nm with the main diameter of 21.06 nm as shown in figure 5. Also, spherical particles within nano ranged from 6.5 nm to 20.0 nm with the main diameter of 12.63 nm as shown in figure 6 which synthesized in the presence of cell-free supernatant of *Streptomyces cyaneus* strain Alex-SK121 and gamma irradiated at 1 kGy. The particle size obtained from DLS measurements is obviously larger than the TEM results because DLS analysis measures the hydrodynamic radius which takes into consideration the all the cell-free supernatant constituents organic layer on the surface of the gold as well [41]. It is evident from the figures (5 & 6) that the biosynthesized gold nanoparticles are spherical in shape and mostly observed as individual particles as well as a few as aggregates. However, nanoparticles were not in direct contact even within the aggregates, indicating stabilization of these particles by a capping agent. The observations led to the suggestion that the release of extracellular proteins such as enzymes in the presence of reducing agent such as melanin pigment as previously mentioned could possibly perform the formation and stabilization of AuNPs in aqueous medium.

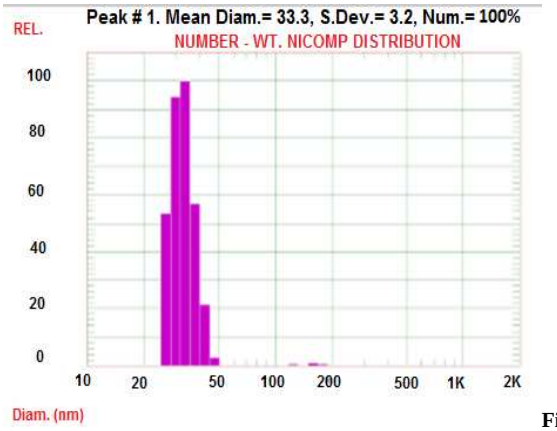

Fig. 3. DLS pattern of particle size distribution of the synthesized AuNPs in the presence of cell-free supernatant of *Streptomyces cyaneus* strain Alex-SK121 heated at 100°C

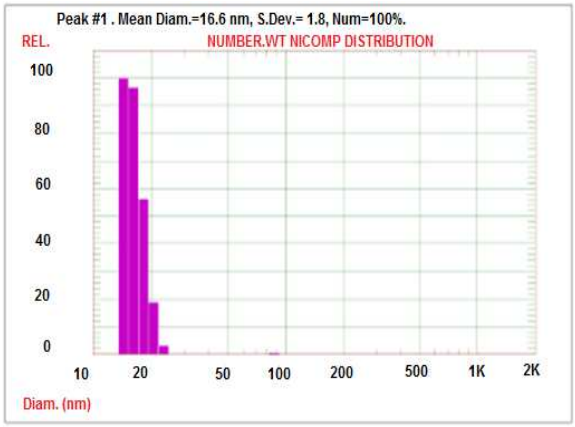

Fig. 4. DLS pattern of particle size distribution of the synthesized AuNPs in the presence of cell-free supernatant of *Streptomyces cyaneus* strain Alex-SK121 gamma irradiated at 1.0 kGy

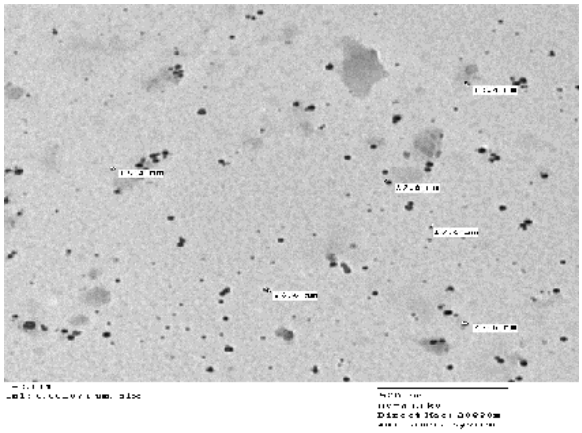

Fig. 5. TEM of the synthesized AuNPs in the presence of cell-free supernatant of Streptomyces cyaneus strain Alex-SK121 and heated at 100°C

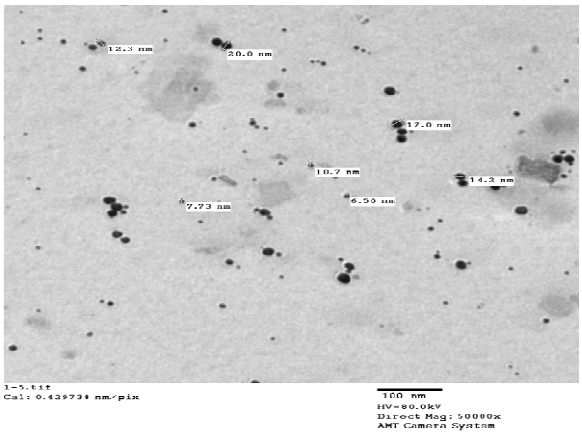

Fig. 6. TEM of the synthesized AuNPs in the presence of cell-free supernatant of *Streptomyces cyaneus* strain Alex-SK121 and gamma irradiated at 1.0 kGy

X-Ray Diffraction (X-RD).

For XRD analysis, the prepared sample was centrifuged and the precipitate was dried under vacuum and taken for XRD analysis. **XRD** was also used to examine the synthesized AuNPs. In XRD, x-rays that are produced by the x-ray beam get scattered by the atoms in the sample. Waves are then scattered spherically from the atoms which causes the intensity of the scattered radiation to show minimum and maximums in different directions. XRD allows a better visual of the structure of the observed atoms because it shows axes, shape, size and position of the atoms. XRD pattern for the gold aggregates is shown in Figure 7, several peaks are observed, these being at Au nanocomposite show the diffraction features appearing at 2 theta (degree) as 38.2◦ , 44.5◦ , 64.7◦ , and 77.6◦ , which correspond to the (111), (200), (220), and (311) planes of the standard cubic phase of Au, respectively. They are identical with those reported for the standard gold metal (Au^0). The obtained data was matched with the Joint Committee on Powder Diffraction Standards (JCPDS), USA, card No. 893722, file no: 01-1174 for Au. The presence of these four intense peaks corresponding to the nanoparticles was in agreement with the Bragg's

reflections of gold identified with the diffraction pattern [19&42]. Thus, the XRD pattern suggests that the gold nanoparticles were essentially in the face-centered cubic (fcc) structure and crystal in nature. The observation of diffraction peaks for the gold nanoparticles indicates that these are crystalline in this size range while its broadening is related to the particles in the nanometer size regime as shown in Fig 7. The mean particle diameter of AuNPs was (31.2 nm), which calculated from the XRD patterns using the following :

Debye –Scherrer's equation: $D = k\lambda / \beta \cos \theta$

The obvious increase in AuNPs size as compared with DLS and TEM data may be due to aggregation of AuNPs during sample preparation for XRD technique.

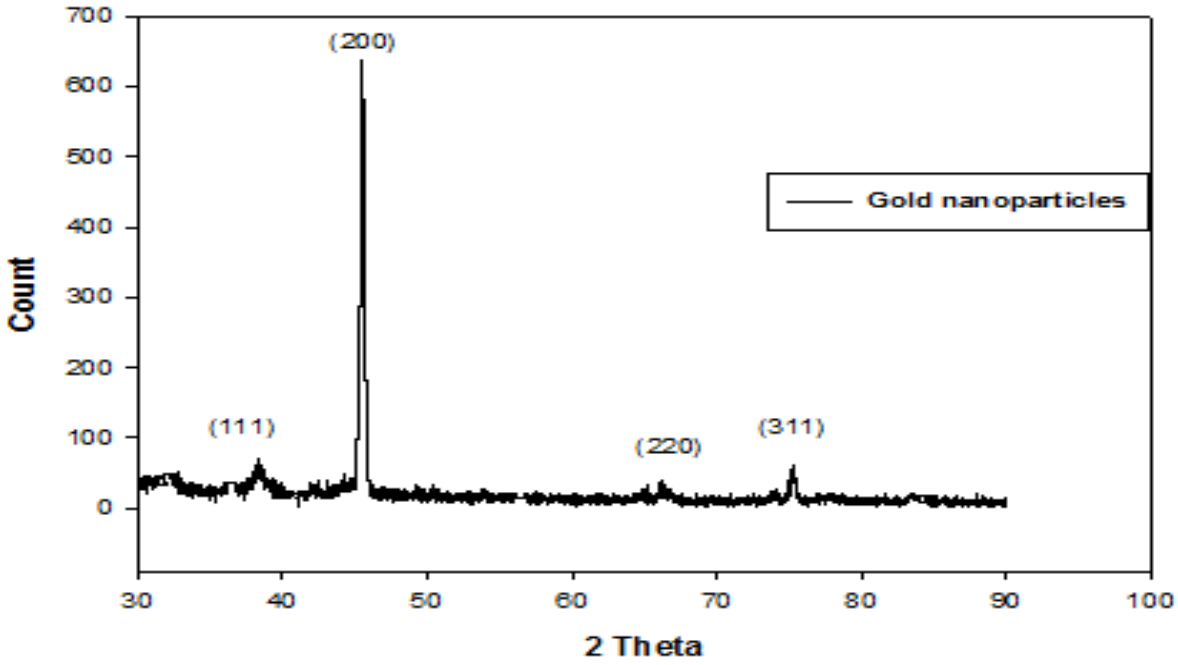

Fig. 7. XRD of the synthesized AuNPs in the presence of cell-free supernatant of *Streptomyces cyaneus* strain Alex-SK121 and gamma irradiated at 1.0 kGy

Fourier Transforms Infrared Spectrometer (FT- IR)

It was observed from the FT-IR spectrum of AuNPs which synthesized by cell-free supernatant of *Streptomyces cyaneus* strain Alex-SK12 heated at 100^{o}C or gamma irradiated at 1 kGy that the bands at 767.53 cm^{-1} corresponding to a primary amine (NH band), and 2025.9 cm^{-1} corresponding to a primary amine (NH stretch vibrations of the proteins) as shown in Fig. 8 and Table 13. Also, a broad absorption band at 3429.80 cm^{-1} indicates the presence of –OH and NH_2 groups and small band at 2346.00 cm^{-1} can be assigned to stretching vibration of aliphatic C-H group. The characteristic band at 1189.9 cm^{-1} attributed to vibrations of aromatic ring C=C of amide I C=O and/or of COO- groups. The positions of these bands were close to that reported for native proteins. The FT-IR results indicate that the secondary structure of proteins was not affected as a consequence of reaction with Au^{+} ions or binding with AuNPs and there are no differences in the position of peaks and slightly changes in %T which indicated that AuNPs incorporated or capped physically by the function group of native protein found in Cell-Free Supernatant of Streptomyces cyaneus strain Alex-SK121 [41].

It is interesting to note that, melanin pigment which responsible for reduction mechanism in AuNPs synthesis found in filtrate of *Streptomyces cyaneus* strain Alex-SK121 and this is indicated by FTIR analysis with a standard melanin pigment [43] which show absorption at 3500 cm^{-1} for standard and for actinomycetal melanin pigment obtained in this study the signals from 3429.8 cm^{-1} and 2853.2 cm^{-1} attributed to the stretching vibrations of (-OH, -NH) the carboxylic, phenolic and aromatic amino functional groups of indolic and pyrrolic systems. The OH bending of phenolic and carboxylic groups are present in 1384.6 cm^{-1} and 1352.8 cm^{-1} in the melanin pigment. These observations seem to indicat that melanin pigment still founded in the filtrate of *Streptomyces cyaneus* strain Alex-SK121**.**

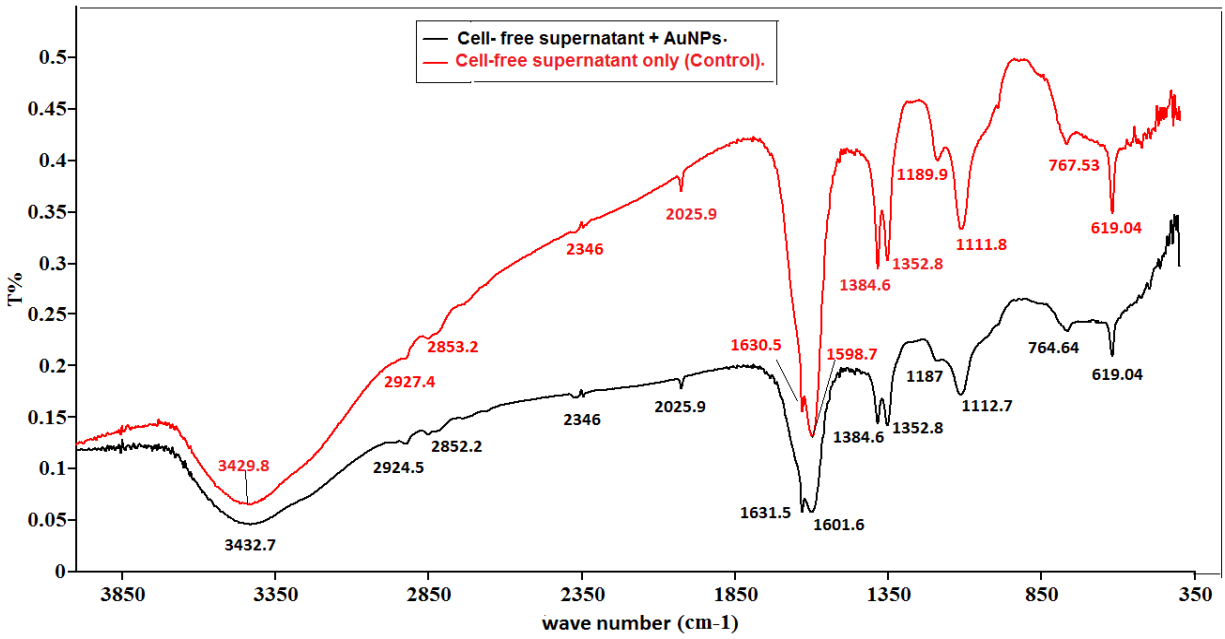

Fig. 8. FT-IR spectrum of fermented extract with gold nanoparticles (Black Peaks) and without gold nanoparticles (Red Peaks)

Table 13. FT-IR Wave number of characteristics bonds and corresponding assignments for *Streptomyces cyaneus* strain Alex-SK121 without and with AuNPs.[7&41]

Peak number	Filtrate Wave number (cm^{-1})	Filtrate +AgNPs Wave number (cm^{-1})	Comment
1	3429.80	3423.70	Corresponding to OH and NH- group band vibration
2	2927.40	2924.50	These peaks are characteristic to the presence of–NH amino group and–OH stretching group in alcoholic and phenolic compounds .The slightly change in T% in this peak may be due to the physical binding or incorporation of Au ions to OH group forming stable AuNPS.
3	2346.00	2346.00	Corresponding to stretching vibration of aliphatic C-H group
4	1189.9	1187.0	May be ascribed for the presence of C=O stretching group, and attributed to vibrations of aromatic ring C=C of amide I C=O and/or of COO- groups.
5	767.53	764.64	Due to N-H in the primary amine.

BIOLOGICAL APPLICATIONS OF THE SYNTHESIZED AuNPs

Antimicrobial Activity

The antimicrobial activity of green synthesized dispersed gold nanoparticles was tested by referring to tetracycline as a standard antibacterial agent and Amphotericin B as a standard antifungal agent (10 µg/disc). As shown in Table 14, the biologically synthesized AuNPs (10 µg/ml) showed good antibacterial activity against Gram- positive and Gram-negative bacteria among the bacterial pathogens tested, maximal growth inhibition was observed for *Bacillus subtilis* and *E.coli*, and also, AuNPs showed antifungal activity against unicellular fungi, when compared to the standard antibiotic. In this connection it may be mentioned that, the AuNPs bind to the bacterial cell membrane and break through bacteria cell wall and interact with protein- and phosphorous-containing compounds, such as DNA. After interaction, AuNPs may attack the respiratory mechanisms, cell division, and finally leads to death. Also, several studies reported that gold ions react with SH groups of proteins and play a vital role in bacterial inactivation. Uncoupled respiratory electron transport from oxidative phosphorylation which inhibits respiratory chain enzymes and interaction with nucleic acids probably results in the impairment of DNA replication. In the present study the antimicrobial ability of AuNPs might be referred to their small size (main diameter of 12.63 nm), which is smaller than the bacteria or fungi. This makes them easier to adhere with the cell wall of the microorganisms causing destruction and leads to the death of the cell. Metal nanoparticles are the damaging agents to bacteria and fungi [19&44&45].

Table 14. Antibacterial and Antifungal activities of AuNPs against some bacterial and fungal test strains as zone of inhibition and MIC

Microorganism	Zone of inhibition (mm)		MIC ppm (µg/ml) AuNPs
	AuNPs	Standard Antibacterial agents(Tetracycline) and Antifungal Agent (Amphotericin B)	AuNPs
Bacillus subtilis ATCC 6633	39±3mm	18±1mm	6.25 µg/m
Staphylococcus aureus ATCC 6538	28±2mm	29±3mm	3.12 µg/ml
Escherichia coli ATCC 7839	33±3mm	32±3mm	6.25 µg/ml
Pseudomonas aeruginosa ATCC 9027	26±2mm	20±2mm	6.25 µg/ml
Candida albicans ATCC 10231	30±2mm	19±1mm	1.25 µg/ml

Therefore, based on the findings of the above reports, it can be assumed that metallic nanoparticles have attracted great interest in their development as potential antimicrobial drugs.

Antioxidant Activity

Numerous essential free radical species are generated in our body during cellular metabolism; those are responsible for cellular signaling, pathogen defense and homeostasis etc. But excessive free radical generation causes damages to the living organisms. For instance, free radical oxygen species attack directly on unsaturated fatty acids in the cell membrane causing damages to the cells. So, in this regard an antioxidant plays a crucial rule. An antioxidant may terminate the oxidative potentiality by scavenging the free radical which is generated during oxidation process. Recently, some progresses have been achieved in the evaluation of antioxidant activity of nano materials [46].

The antioxidant activity of the synthesized AuNPs was evaluated using DPPH (2,2-diphenyl-1-picrylhydrazyl) scavenging assay. DPPH is a stable nitrogen-centered free radical, the color of which changes from violet to yellow upon the reduction by either the process of hydrogen or electron donation. Substances which are able to perform this reaction can be considered as antioxidants and, therefore, radical scavengers. As shown in Table 15, a significant difference was observed among the respective values obtained. The DPPH values were increased in a dose dependent manner. Gold nanoparticles (AuNPs) are one of the most commonly used nanomaterials. Gold nanoparticles possessing antioxidant activity against various in vitro antioxidant systems. The free radical scavenging activity of AuNPs was found to be high as compared with standard, which confirmed in the present investigation. From the above assays, the possible mechanism of antioxidant activity of AuNPs includes reductive ability, electron donating ability and scavengers of radicals. Among various metal nanoparticles, Au nanoparticles are well-suited for a wide range of biological applications because of its chemical inertness and resistance to surface oxidation . The surfaces of Au nanoparticles are particularly suitable to serve as a stable and non-toxic platform, on which pharmaceutical compounds can be delivered [19&47].

Table 15. DPPH Free radical scavenging activity of biosynthesized gold Nanoparticles and Tert-Butyl hydroquinone (TBHQ) (Stander)

Concentration AuNPs/ TBHQ (ppm)	Absorbance λ (517nm)		Scavenging activity %	
	AuNPs	TBHQ	AuNPs	TBHQ
5.0	0.28	0.30	66	70
10.0	0.18	0.21	75	79
20.0	0.12	0.14	83	86
40.0	0.07	0.11	90	89
80.0	0.03	0.02	96	98

Antitumor Activities

Nanoparticles as AuNPs are usually smaller than several hundred nanometers in size, comparable to large biological molecules such as enzymes, receptors, of a size about 100 to 10,000 times smaller than human cells. These nanoparticles can offer unprecedented interactions with biomolecules both on the surface and inside the body cells, which may bring revolution in cancer diagnosis and treatment [48]. The biosynthesized gold nanoparticles (AuNPs) exhibited antitumor activity against human breast carcinoma cells MCF7 (ATCC HTB22) and human liver carcinoma cells HEPG-2 (ATCC HB8065) with IC_{50} 64.3 and 76.7 µg/ml, respectively. Data are represented in (Figure 9 for MCF7 (ATCC HTB22) cell line) and (Figure 10 for HEPG-2 (ATCC HB8065) cell line. While the cytotoxicity biosynthesized gold nanoparticles (AuNPs) on non-tumor cells have IC_{50} 433.2 µg/ml (Figure 11). Dreaden *et al.*,[49], reported that gold nanoparticles present tremendous opportunities for the design of next-generation, multimodal anti-cancer treatment strategies involving photothermal therapy, drug delivery, gene therapy, and cell cycle regulation. Also, in this connection it may be mentioned that, the cellular uptake, cytotoxicity, and subcellular localization of AuNPs are highly sensitive to the particle size, shape, surface charge, hydrophobicity, and nature of the surface ligands. AuNPs caused hydrogen oxygen accumulation by cytosolic glutathione (GSH) depletion and subsequently activated mitochondrial apoptosis pathway. Also, AuNPs localizing in cell nuclei would induce DNA damage and cytokinesis arrest as reported in [50&51]. The most exciting aspect of the particles was their instant effect on cancer cell lines and their non-toxicity towards normal cells. Breast cancer is

the most common and the second leading cause of cancer death among women. In the present study, we showed that MCF-7 breast cancer cells treated with gold nanoparticles significantly reduced and may be helpful in overcoming some of the challenges inherent to current breast cancer treatment modalities.

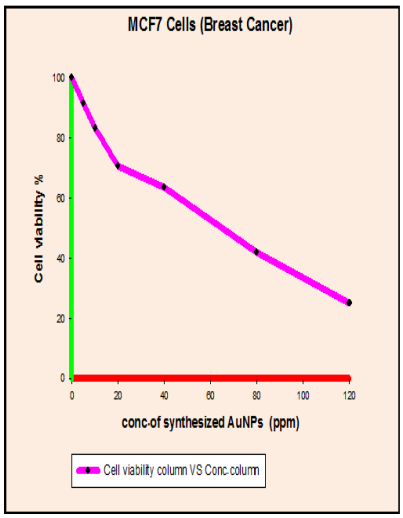

Figure 9. Antitumor activity of synthesized AuNPs against MCF7 (ATCC HTB22) cell line

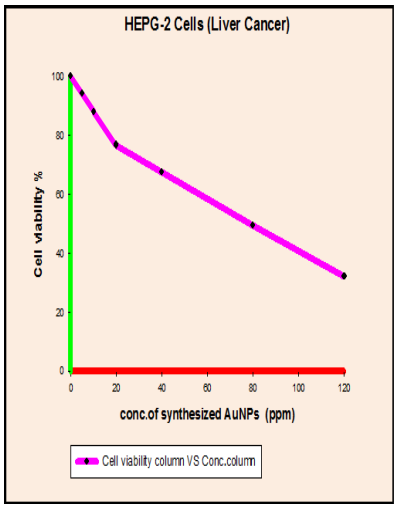

Figure 10. Antitumor activity of synthesized AuNPs against HEPG-2 (ATCC HB8065) cell line

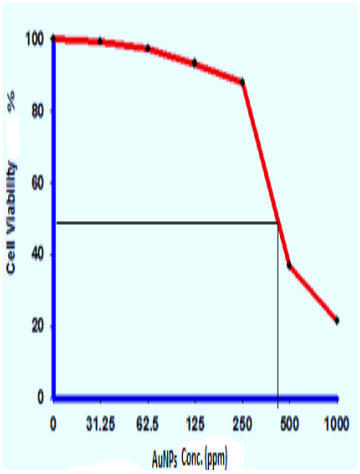

Figure (11): Cytotoxicity assay of gold nanoparticles on the normal cell line (non tumor cell line)

CONCLUSION

Marine ecosystem is still an unexplored estuarine habitat of its rich microbial diversity. There are huge possibilities for the occurrence of potential microbes to withstand metal stress in its nutrient rich habitat. With this background, we have isolated a unique *Streptomyces cyaneus* strain Alex-SK121and studied its capability to synthesize AuNPs using different gamma irradiation doses and under action of heat. The synthesized gold nanoparticles were characterized by UV–Visible, DLS, TEM, X-RD and FTIR spectroscopy. Also, the different biological activities of the AuNPs were evaluated. The synthesized gold nanoparticles may be advantageous as antimicrobial agent against a range of pathogenic bacteria and fungi. The AuNPs also show promise as antitumor agents containing some level of antioxidant activity.

Acknowledgement
The authors are wish to acknowledge the Drug Radiation Research Department, National Center for Radiation Research and Technology (NCRRT), Cairo, Egypt, and Biology Department, Collge of Science, Qassim University, Saudi Arabia, for providing facilities for the execution of the research work to complete successfully.

REFERENCES

[1] L Karthik ; G Kumar ; AV Kirthi ; AA Rahuman ; KVB Rao. *Bioprocess Biosyst. Eng.*, **2014**, 37,261–267.
[2] S Tikariha; S Singh; S Banerjee; A S Vidyarthi. *International J. Pharmac. Sci. Research.* , **2012**, 3(6), 1603-1615.
[3] H Shiying; G Zhirui; Y Zhanga; S Zhanga; J Wanga; G Ning. *Mater Lett.*, **2007**, 61,3984–3987.
[4] K Kathiresan; S Manivannan; M Nabeel; B Dhivya. *Coll. Surf. B.*, **2009**, 71,133–137.
[5] M Hsiao; S Chen; D Shieh; C Yeh. *J. Phys. Chem. B.* , **2006**, 110,205 -210.
[6] A Ahmad; S Senapati; M Islam Khan; R Kumar; M Sastry. *Langmuir*, **2003**, 19 (8), 3550–3553.
[7] A I El-Batal; M H El-Sayed; B M Refaat; A A Z Askar. *British J. Pharmac. Res.* , **2014**, 4(21), 2525-2547.
[8] P Velmurugan; M Iydroose; MH Mohideen; TS Mohan; M Cho, BT Oh. *Bioprocess Biosyst. Eng.* **2014**, 37(8),1527–1534.
[9] P Manivasagan; J Venkatesan; K Sivakumar; SK Kim. *Crit. Rev. Microbiol.*, **2014** , 28,1-13.
[10] SM Ghaseminezhad; S Hamedi; SA Shojaosadati. *Carbohyd. Polym.* ,**2012**, 89,467–472.
[11] VC Verma; R.N. Kharwar ; AC Gange. *CAB Rev. Perspect. Agric. Vat. Sci. Nutr. Nat. Resour.*, **2009**, 4(26), 1-17.
[12] V Gopinath; D MubarakAli; S Priyadarshini; NM Priyadharsshini; N Thajuddin; P Velusamy. *Coll. Surf. B Biointerfaces*, **2012**, 96, 69–74.
[13] SV Otari ; RM Patil; NH Nadaf ; SJ Ghosh ; SH Pawar . *Materials Letters*, **2012**, 72, 92–99.

[14] P Manivasagan; J Venkatesan; K Senthilkumar; K Sivakumar; SK Kim. Biomed. Res. Int. , **2013**, 287638**,** 1–9.
[15] T Shanmugasundaram; M Radhakrishnan; V Gopikrishnan; R Pazhanimurugan; R Balagurunathan. *Coll. Surf. B Biointerfaces*, **2013**, 111,680–687.
[16] E B Shirling; D Gottlieb. *Int. J. Syst. Bacteriol*., **1966**, 16, 313-340 .
[17] A Tadashi.*The Society for Actinomycetes. Japan. National Agricultural Library*, **1975**, 1,1-31.
[18] AI El-Batal; A M Hashem; N M Abdelbaky. *World Appl. Sci. Journal* ,**2012**, 19 (1): 01-11.
[19] AI El-Batal; A M Hashem; N M Abdelbaky. *SpringerPlus*, **2013**, 2:129, pp.1-10.
[20] AI El-Batal; R Al-Habib. *J. Food, Agricul. & Environ*. **2014**, 12 (2) , 1 4 1 - 1 4 9 .
[21] AI El-Batal; NM ElKenawy; A S Yassin, M A Amin. *Biotechnology Reports*, **2015**, 5, 31–39.
[22] K Tarangini; S Mishra. *Res. J. Engin. Sci*., **2013**, 2(5), 40-46.
[23] JG Cappuccino; N Sherman. Microbiology ,Laboratory Manual. India: Pearson Education, Inc. New Delhi, **2004**; 282–283.
[24] AW Bauer; WMM Kirby; JC Sherris ; M Truck. *American J. Clin. Pathol*., **1966**, 45(4), 493-496.
[25]CLSI, Performance Standards for Antimicrobial Susceptibility Testing, Eighteenth Informational Supplement 18th ed., Clinical and Laboratory Standard Institute, USA **2008;** (ISBN-13: 9781562386535).
[26] AI El-Batal; MA Amin; MMK Shehata; MMA Hallol. *World Appl. Sci. J.* , **2013**, 22 (1), 1-16.
[27] Q Zeng; D Shao; W Ji; J Li; L Chen; J. Song. *Toxicology Reports*, **2014**, 1, 137–144.
[28] C Spatz. Basic Statistics, 5th edn., Brooks/Cole Publ. Co., California, USA, **1993**, 135-161.
[29] J Martin; J Luengo; G Revilla; J Villanueva. Biochemical Genetics of the β-lactam Antibiotic Biosynthesis. In: O Sebek & A I Lskin, (eds.) ,Genetics of Industrial Microorganisms, American Society for Microbiology, Washington. **1979**.
[30] J Martín; A Demain. *Microbiol. Rev*., **1980**, 44, 230-251.
[31] Z Sathi; AM Abdu-Rahman; M Gafur. *Pakist. J. Biol. Sci*., **2001**, 4 (12), 1523-1525.
[32] P James; C Edwards; M Dawson. *J. Gen. Microbiol.* , **1991**,137, 1715–1720.
[33] Q Song ; Y Huang ; H. Yang. *J. Agri. Sci.* , **2012**, 4, (7), 95-102.
[34] J Spizek; P Tichy. *Floia Microbiol*., **1995**, 40(1), 43–50.
[35] Y Aharonowitz; A Demain. *Antimicrob. Agents Chemother*., **1978,** 14(2), 159-164.
[36] G Hobbs; M Catherine; C Frazer; C David; F Gardner; S Oliver. *J. Gen. Microbiol*., **1990**, 136, 2291-2296.
[37] JL Doull; LC Vining. *Biotechnol Adv*., **1990**, 8(1), 141–158.
[38] A Gole; C Dash; V Ramakrishnan; SR Sainkar; AB Mandale; M Rao; M Sastry. *Langmuir*, **2001**, 17, 1674–1679.
[39] M A Faramarzi; H Forootanfar. *Colloid. Surf. B*, **2011**, 87, 23–27.
[40] AI El-Batal; AF El-Baz; FM Abo Mosalam; AA Tayel. *J. Chem. Pharmac. Res*., **2013**, 5(8), 1-15.
[41] AI El-Batal; B M. Haroun; A A Farrag; A Baraka; G S. El-Sayyad. *British J. Pharmac. Res*., **2014**, 4(11), 1341-1363.
[42] S BarathManiKanth; K Kalishwaralal; M Sriram; S Ram Kumar Pandian; H Youn; S Eom; S Gurunathan. *J. Nanobiotech*., **2010**, 8, 16 ,1-15.
[43] K Tarangini; S Mishra. *Biotechnology Reports*, **2014**, 4, 139–146.
[44] A Chwalibog; E Sawosz; A Hotowy; J Szeliga; S Mitura; K Mitura; M Grodzik; P Sokolowska . *Int. J. Nanomed*., **2010**, 5, 1085–1094.
[45] P Prakash ; M Anita ; P K Poornima. *Appl. Nanosci*., **May 2015,** pp, 1-7.
[46] S Sharma; A K Manhar; P J Bora; S K Dolui; M Mandal. Adv. Mater. Lett., **2015**, 6(3), 235-241.
[47] NN Duya; DX Dub; DV Phua; LA Quoca; BD Duc; NQ Hiena. *Colloids and Surfaces A: Physicochem. Eng. Aspects*, **2013**, 436, 633– 638.
[48] R Seigneuric; L Markey; DSA Nuyten; C Dubernet; CTA Evelo; E Finot; C Garrido. *Curr. Mol. Med.*, **2010**, 10, 640–652.
[49] EC Dreaden; M A Mackey, X. Huang, B Kang; MA El-Sayed. *Chem. Soc. Rev*., **2011**, 40, 3391–3404.
[50] B Kang; MA Mackey; MA El-Sayed. *J. Am. Chem. Soc*., **2010**, 132 , 1517–1519.
[51] W Gao; K Xu; L Ji; B Tang. *Toxicol. Lett*., **2011**, 205, 86–95.